Table of Contents

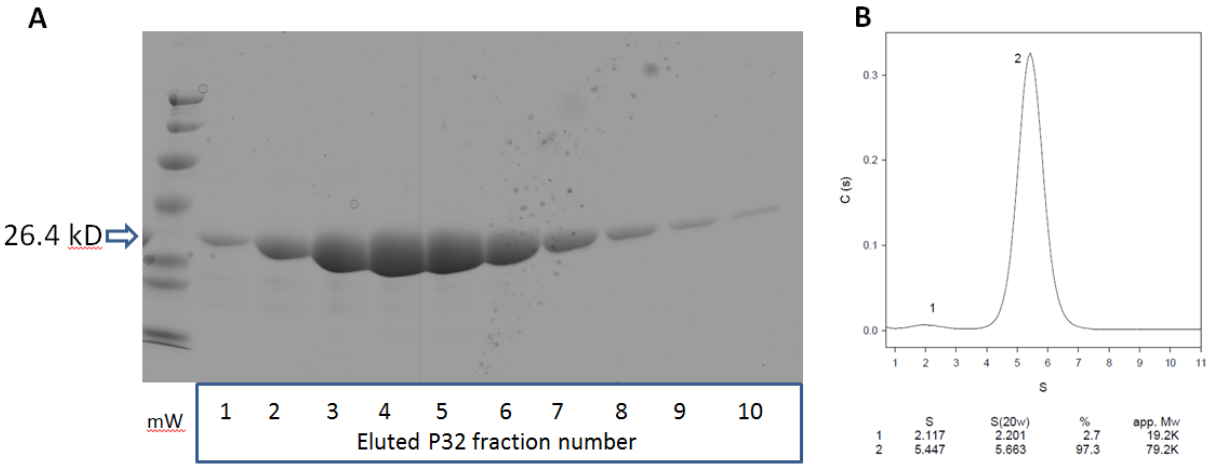

Supplemental Figure 1. Purification and oligomerization analysis of the of p32 protein. (A) 6x-His-Tagged P32 was expressed in Rosetta-gami-2 cells (Novagen). The protein was purified by IMAC using HIS-select resin (Sigma) with an imidazole gradient from 20-300 mM and eluted fractions were analyzed on analytical SDS-PAGE. (B) Sedimentation velocity assay that allows determination of the multimeric state of proteins demonstrated that similarly to the native p32 protein, recombinant p32 is present predominantly (>97%) as a trimer with sedimentation coefficient of 5.447 and an apparent molecular weight of complex 79.2 kDa.

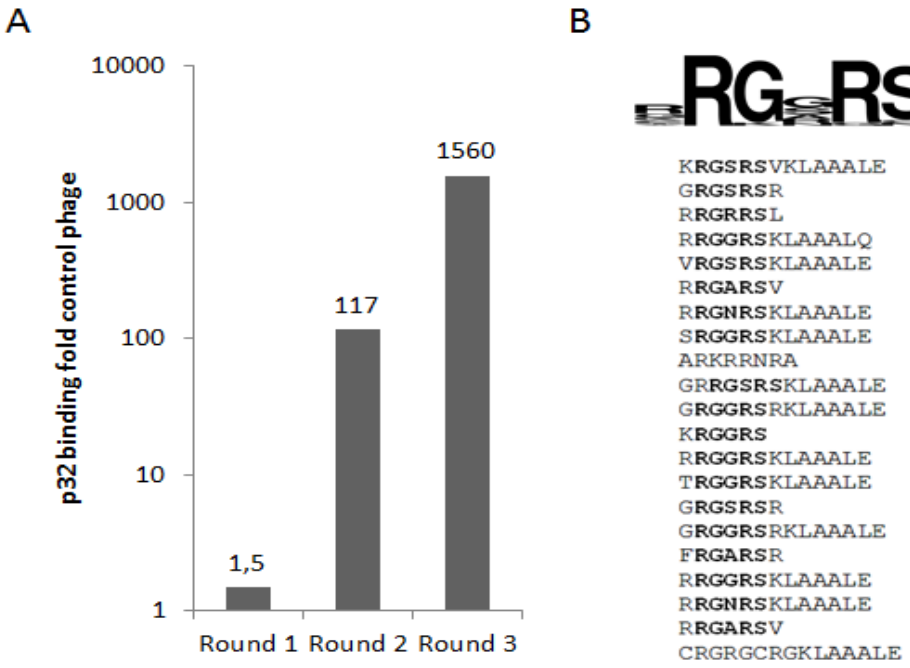

Supplemental Figure 2. Screening of T7 X7 libraries.

(*A*) X7 peptide library was used for *in vitro* selection on his-tagged recombinant p32 protein immobilized on Ni-NTA magnetic beads. Binding of phage particles in each selection round is expressed fold control phage displaying heptaglycine control peptide (G7). *(B)* Representative peptide sequences recovered after three rounds of *ex vivo* selection. Note emergence of RGXRS consensus motif (bold) in selected peptide pool.

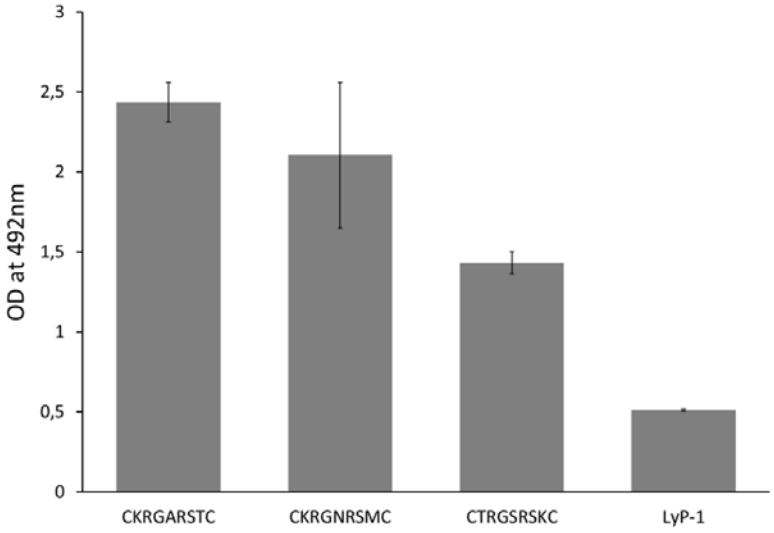

Supplemental Figure 3. Binding of novel peptide-expressing phages to p32 protein. The affinity of novel peptide-expressing phages to p32 was tested in ELISA-type of assay and compared to phages expressing known p32-binding peptide, Lyp-1. Phages were incubated on p32-coated plate, followed by treatments with polyclonal rabbit anti-T7 antibody, HRP-labeled anti-rabbit IgG, and OPD silver and gold substrate for color reaction. Phage binding to p32 was detected by measuring the absorbance. Error bars represent average ± S.D., n=4-6.

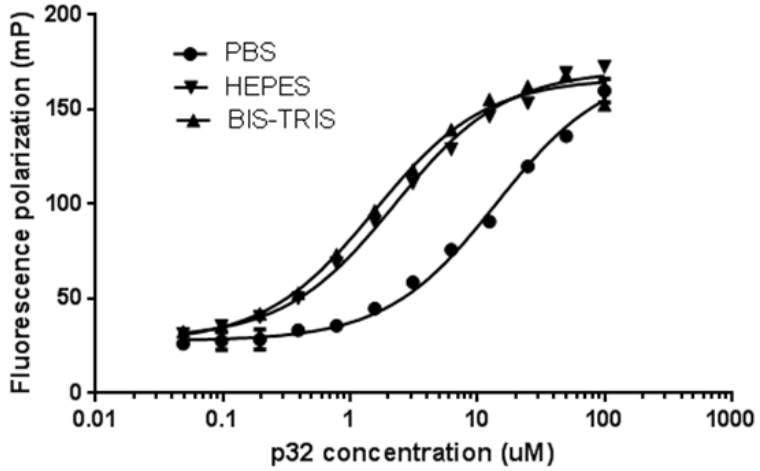

Supplemental Figure 4. Effect of buffer solution on interaction of TT1 and p32. The binding affinity of FAM-labeled TT1 to p32 was studied in different assay buffers: in PBS, HEPES, and BIS-TRIS, respectively. The binding was measured by fluorescence polarization (FP) and observed as increased FP value. Binding constants (K_D) were calculated by fitting the binding curves into Michaelis-Menten kinetics. Each data point presents average ± S.D., n=4-6.

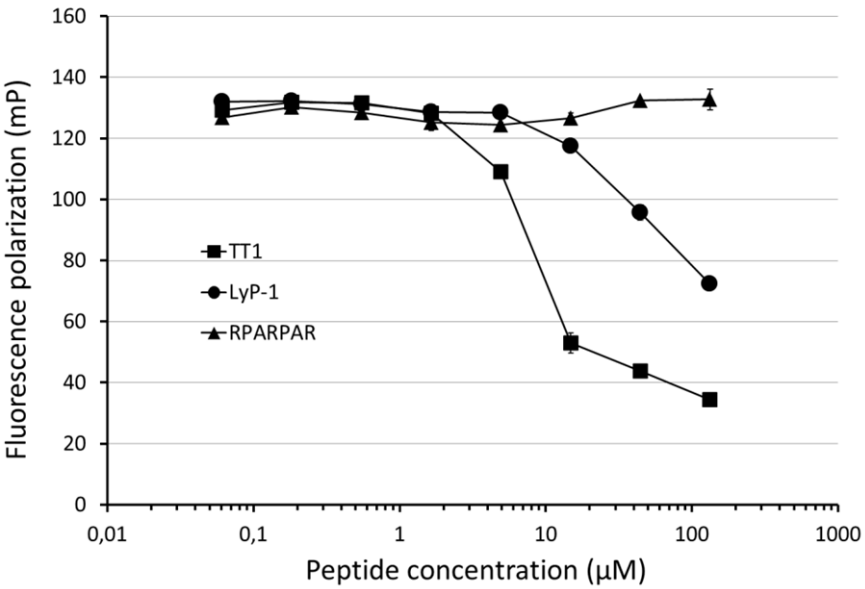

Supplemental Figure 5. Specificity of the FAM-TT1 binding to p32. Dislocation of FAM-TT1 from p32 with unlabeled peptides was studied to check the specificity of TT1-p32 interaction. FAM-TT1 and p32 were incubated together with unlabeled TT1 and LyP-1, and unlabeled RPARPAR, respectively. Unlabeled TT1 dislocated FAM-TT1 from p32. Known p32 binding peptide, LyP-1, dislocated FAM-TT1 at high concentrations. RPAPAR peptide did not dislocate FAM-TT1, suggesting specific binding of FAM-TT1 to p32. Each data point presents average ± S.D., n=4-6.

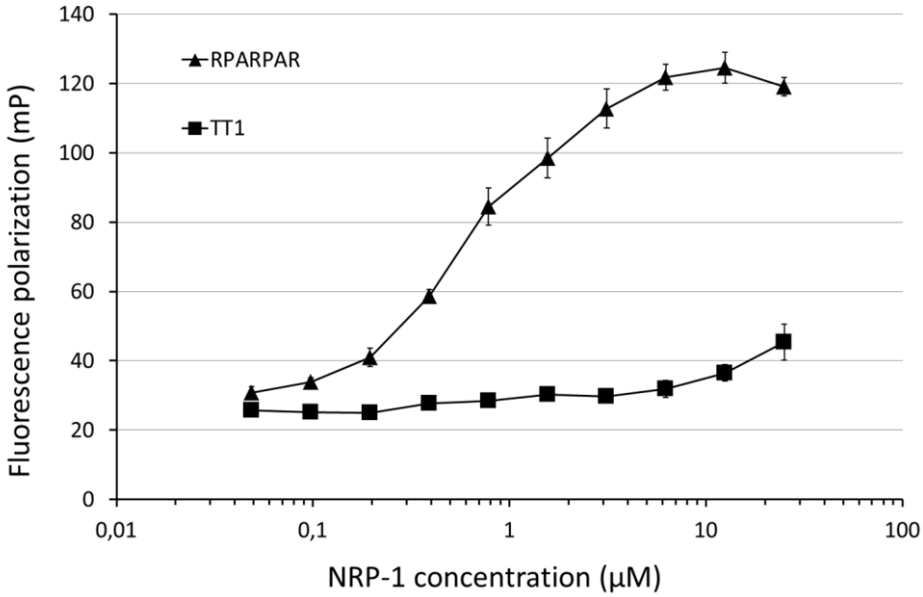

Supplemental Figure 6. Further specificity study of FAM-TT1. Specificity of TT1 was further evaluated by measuring the binding of FAM-TT1 to recombinant non-target protein, b1b2 domain of neuropilin-1 (NRP-1). The binding was studied by fluorescence polarization. FAM-TT1 did not show

binding to NRP-1, where known NRP-1 binding peptide, RPARPAR, showed strong affinity to NRP-1. Each data point presents average ± S.D., n=4-6.

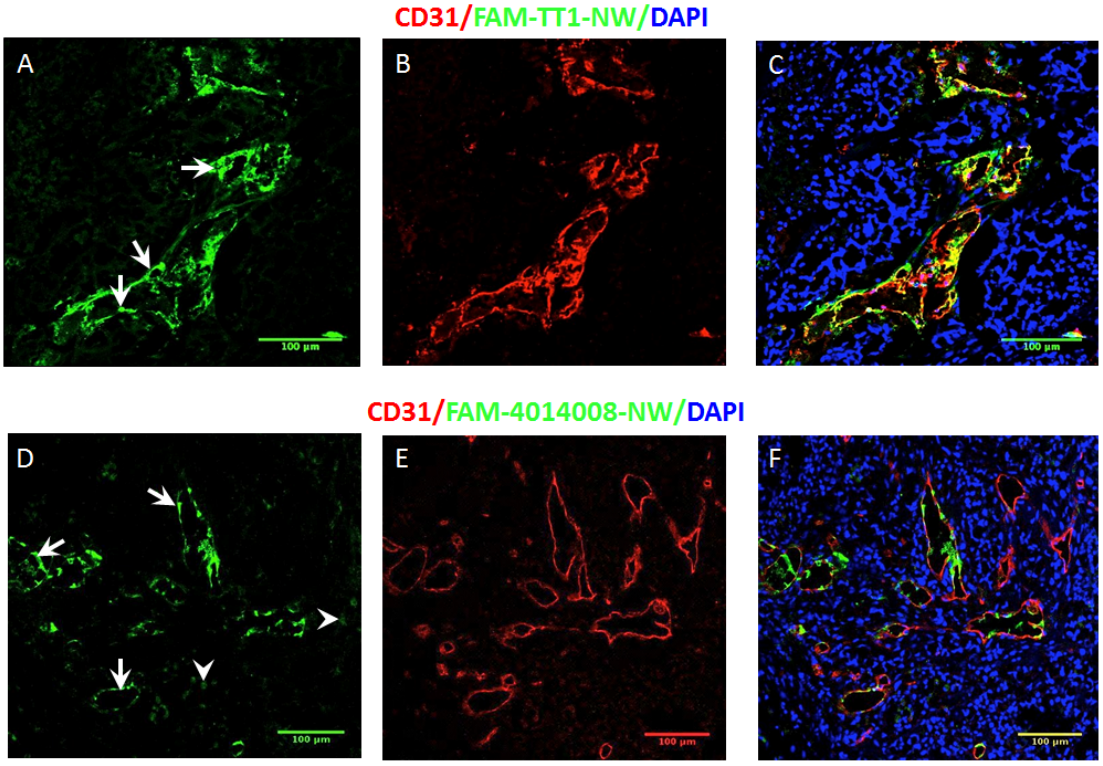

Supplemental Figure 7. *In vivo* homing of TT1 and ##4014008 nanoworms to breast tumors.

(A-C) Confocal imaging of tissue sections of MCF10Ca1A breast tumors from mice injected with FAM-TT1 -IONW. FAM labeled TT1-NWs were injected into the tail vein (7.5 mg of iron per kilogram of body weight) of tumor-bearing mice. The mice were euthanized 5-6 hours after the injection by cardiac perfusion with PBS under anesthesia, and organs were dissected and analyzed for particle homing. Red: CD31; green: IONW; blue: nuclei. **(D-F)** Confocal imaging of tissue sections of MCF10Ca1A breast tumors from mice injected with FAM-##4014008 -IONW . Red: CD31; green: IONW; blue: nuclei.

Arrows point to vascular structures that show co-localization of nanoparticle and p32 signals. Representative fields from multiple sections of three independent mice are shown. Scale bars = 100µm.

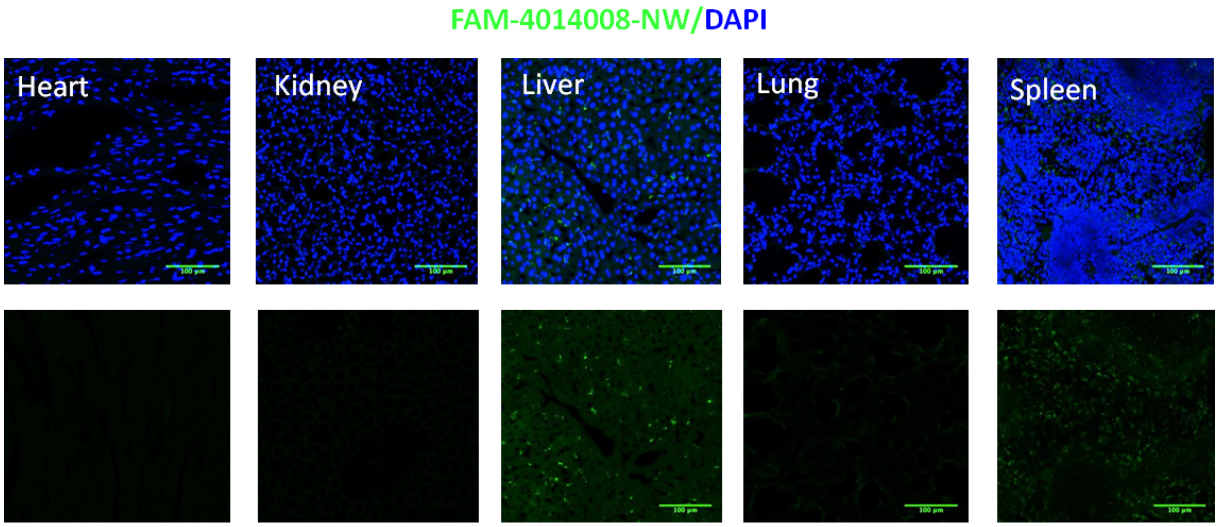

Supplemental Figure 8. *In vivo* distribution of ##4014008 nanoworms in control organs.

Confocal imaging of tissue sections of control organs from MCF10Ca1A breast tumor-bearing mice injected with FAM-##4014008 -IONW . Green: IONW; blue: nuclei. Some nanoparticle uptake is seen in the liver and spleen. Representative fields from multiple sections of three independent mice are shown. Scale bars = 100 µm.

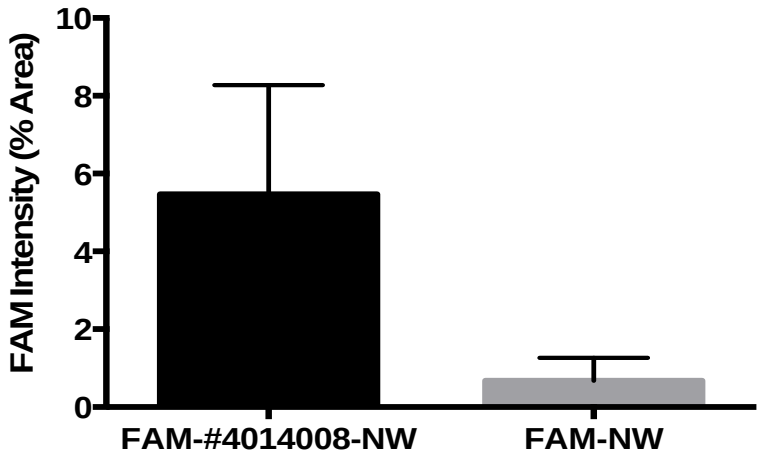

Supplemental Figure 9. Quantification of *in vivo* homing of NW functionalized with compound #4014008 and with a control peptide ARAL.

NWs were coated with either #4014008 or FAM, intravenously injected into mice bearing orthotropic MCF10Ca1A breast tumor xenografts. The dose was 7.5 mg/kg body weight of NW iron. The NWs were allowed to circulate for 5 hours, and the mice were perfused through the heart with PBS, and tumors and organs were collected. Quantification of fluorescence was done with ImageJ software ($P<0.0001$, Student's t-test).

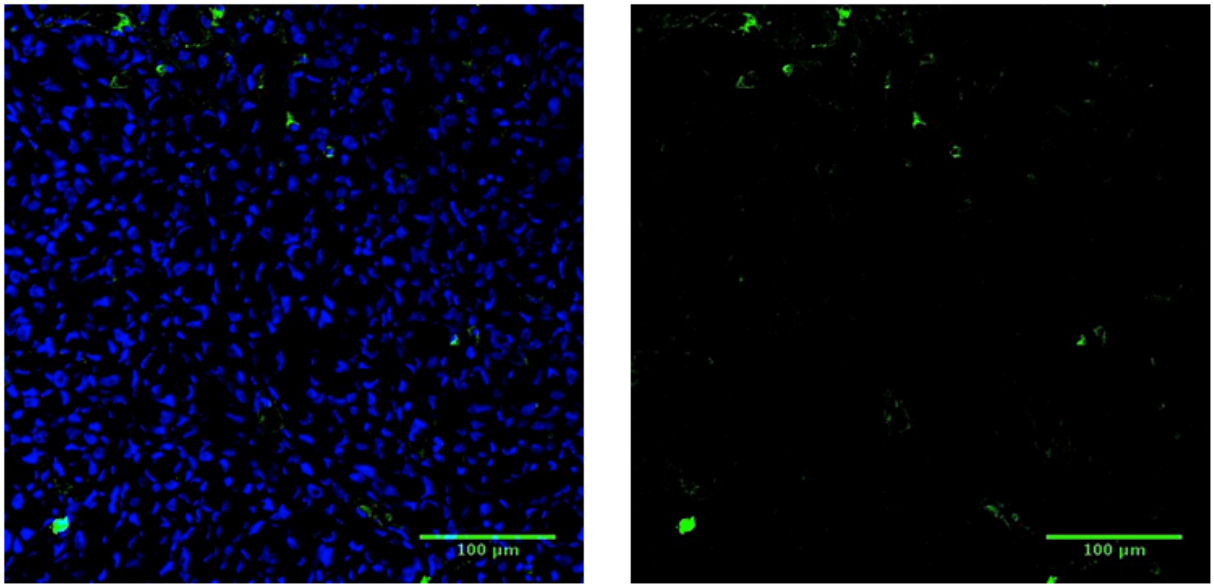

Supplemental Figure 10.

Distribution of control FAM-labeled ARAL-NW in orthotopic MCF10Ca1A breast tumors.

NWs were coated with FAM and ARAL peptide and intravenously injected into mice bearing orthotropic breast tumors. The dose was 7.5 mg/kg body weight of NW iron. The NWs were allowed to circulate for 5 hours, and the mice were perfused through the heart with PBS, and tumors and organs were collected, and sectioned for confocal imaging. Representative fields from multiple sections of three independent mice are shown. Scale bars = 100 µm.

SI-1: Screening protocol and plate layout

FAM-TT-1 and p32 solutions are prepared just before experiment, and stored on ice during the screen; the peptide is shielded from light.

1. Dispense 37.5 nL DMSO into columns 1-4 and 45-48 of assay plate (Corning #3724)
2. Dispense 1.5 µL of assay buffer (50mM BIS-TRIS pH 7.4, 0.05% Tween 20, 1 mM DTT) into columns 1-4
3. Dispense 1.5 µL of p32 protein (12 µM) into columns 5-48
4. Dispense 37.5 nL of compounds (2 mM) into columns 5-44
5. Spin plate
6. Incubate 20 min at room temperature
7. Dispense 1.5 µL FAM-TT-1 peptide (20 nM) into all columns
8. Shake plate and spin plate
9. Incubate 25 min
10. Read plate on PheraStar FS

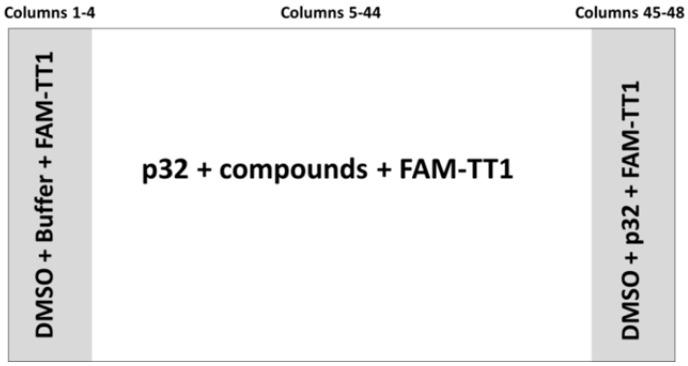

S2: Structures and properties of the hit compounds from p32 FP screening.

Inhibition %	Compound ID	Name	Structure	MW	LogP	PSA	H Bond Donor	H Bond Acceptor	Rotatable Bond
40.5	7933989	(5,5-dimethyl-4,5-dihydro-1,3-thiazol-2-yl){2-[(5,5-dimethyl-4,5-dihydro-1,3-	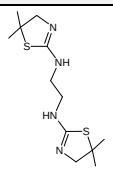	286	0.97	48.8	2	2	5
39.5	6367577	7-hydroxy-8-methyl-4-(trifluoromethyl)-2H-chromen-2-one	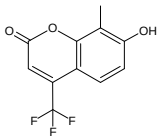	244	3.02	50.4	1	3	0
30.8	88361068	1-{3-amino-6-[4-methyl-2-(1H-pyrazol-1-yl)phenyl]pyrazin-2-yl}pyrrolidin-3-	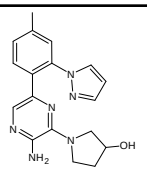	336	2.6	93.1	2	4	3
29.9	4014008	N-(3-methylpyridin-4-yl)ethane-1,2-diamine	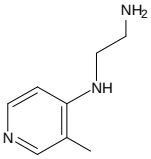	151	0.93	50.9	2	2	3
29.4	54778828	4-{3-[1-(3-pyridinylmethyl)-4-piperidinyl]-1-pyrrolidinyl}-2-pyrimidinami	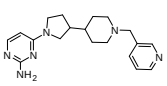	338	2.08	71.2	1	4	4
22.5	91984046	3-(3,4-difluorophenyl)-5-methyl-4,5,6,7-tetrahydroisoxazolo[4,5-	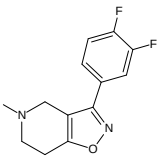	250	2.14	29.3	0	3	1
20.7	9132086	2-methyl-6-(2-thienyl)-6,7-dihydro[1,2,4]triazolo[5,1-b]quinazolin-8(5H)-one	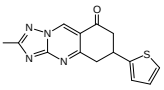	284	1.89	60.2	0	4	1

Experimental Section

Peptides and proteins

Peptides were synthesized as previously described [1]. Briefly, peptides were synthesized using Fmoc/t-Bu chemistry on a microwave assisted automated peptide synthesizer (Liberty, CEM Corporation). Peptides were purified by HPLC using 0.1% TFA in acetonitrile-water mixtures to 90%-95% purity and validated by Q-TOF mass spectral analysis. Fluorescent peptides were synthesized by using 5(6)-carboxyfluorescein (FAM) with 6-aminohexanoic acid spacer to keep the fluorescent dye further away from the peptide. Proteins p32 and NRP-1 were obtained from Sanford-Burnham-Prebys Medical Discovery Institute (SBP) Protein Production and Analysis Facility (La Jolla, CA).

T7 phage peptide library biopanning

In vitro T7 peptide phage biopanning was used to identify peptides binding to p32 protein, as described earlier [2] . Briefly, T7-select phage display system (EMD Biosciences, Gibbstown, NJ, USA) with T7 vector 415-1b was used to construct cyclic CX7C phage libraries (diversity – 10^8) and for individual phage cloning according the manufacturer's instructions. Phage was amplified in E. coli (BLT5403, EMD Biosciences, Gibbstown, NJ, USA), purified by precipitation with PEG-8000 (Sigma-Aldrich, St. Louis, MO, USA) followed by $CsCl_2$ gradient ultracentrifugation and dialysis [2]. Library selections were performed on the recombinant hexahistidine –tagged p32 coated on Ni-NTA magnetic beads (Qiagen, Hilden, Germany) in washing buffer (PBS containing 0,05% Tween-20, 5mM imidazole and 0.5% BSA, pH-7.4). 10^8 phage particles were incubated in 0.5 mL of the buffer for 1hr followed by 4 washes and elution of protein-phage complexes in PBS containing 400mM imidazole. Phage was quantified using plaque assay and the sequences of phage-displayed peptides were inferred from the DNA encoding the insert-containing region at the C-terminus of the T7 major coat protein gp10.

Phage binding assay

The binding of individual phage to p32 was verified using ELISA-type of phage binding assay. 96-well plates (Corning Life Sciences, Tewksbury, MA, USA) were coated with 100µL of 5µg/mL p32 in PBS at 4°C overnight, washed 3 times with 200 µL of PBST (PBS + 0.05% Tween-20), blocked with 200 µL of 0.5 % bovine serum albumin (BSA) in PBST for 1 h at 37°C, and washed 3 times with PBST. Phages ($1.11*10^8$ pfu in 100 µL PBST) were added to

p32–coated/BSA –blocked wells, the plate was incubated at 4°C overnight, and washed 3 times with PBST. Subsequently, the plates were incubated with 100 µL in-house prepared polyclonal rabbit anti-T7 antibody diluted 1:1000 in PBST for 1h at 4°C, and washed 3 times with washing buffer. Horseradish peroxidase (HRP)-labeled anti-rabbit IgG (Sigma-Aldrich) was diluted 1:1000 in PBS, and 100 µL was added to the wells, followed by 1h incubation at 4°C and washing 3 times. Next, 100 µL of OPD silver and gold substrate (Sigma-Aldrich) was added to the wells and incubated at room temperature until visible color was observed (<30 min). The reaction was stopped by adding 50 µL of 1M H_2SO_4, and the plate was read at 492nm (Varioskan Flash, Thermo Scientific, Waltham, MA, USA).

Fluorescence polarization assay

Fluorescence polarization (FP)–based assay was used for solution-based screening of compound libraries for p32 binding compounds. FP assays have been used in high-throughput screening in drug discovery process since mid-1990's [3]. In FP assays, peptide conjugated with a fluorescent label (fluorescein-AM, FAM) is excited with polarized light. Free peptide in solution rotates fast and the polarization of emitted light differs from excitation plane, which is observed as low polarization (SI Fig 1A). When peptide binds to larger molecule, such as receptor protein, the rotation decreases significantly and emitted light retains its incident polarization (SI Fig 1B). Fluorescence polarization is given as milli-polarization (mP) value, which is obtained from equation (1):

$$mP = 1000*(S-P)/(S+P),$$

(Eq. 1)

where S is fluorescence parallel to excitation plane and P is fluorescence perpendicular to excitation plane [4] .

The assay was initially set up in 20 µLwell final volumes in 384 well plates (Corning Life Sciences) , and measurements were carried out using PheraStar FS plate reader (BMG LABTECH, Ortenberg, Germany) in quadruplicate. Peptide and protein stock solutions were diluted to desired concentration with assay buffer (50 mM BIS-TRIS pH 7.4, 0.05% Tween20, 1 mM DTT). FAM-labeled peptides were protected from light during the experiment to avoid photobleaching. Optimal concentration of fluorescein (FAM) labeled-peptides for the assay was determined by measuring the limit of detection (LOD), signal-to-background ratio (S/B), and stability of mP value over series of peptide concentrations. In the

binding assay, the concentration of FAM-peptide was kept constant, and the FP was measured over the range of target protein concentrations. The peptide dissociation constant (K_D) was obtained by fitting the binding curve into Michaelis-Menten kinetics in GraphPad Prism– software (GraphPad Software, Inc., CA, USA). The specificity of the binding assay was confirmed by the displacement assay, in which FAM-labeled peptide was competed off from the target protein by titrating the unlabeled peptide up to 100 μM, and by testing the binding of the peptide to b1b2 domain of NRP-1 (Vander Kooi et al., 2007; Teesalu et al., 2009).

High-throughput screening

Fluorescence polarization assay was transferred to 1536-well plate format using volumes and concentrations listed in Table 1. The detailed screening protocol including negative and positive controls is presented in supplementary material (S1). Chemical library of ~50,000 compounds from ChemBridge (San Diego, CA) was screened in High-Throughput Screening Facility at *Conrad Prebys* Center for Chemical Genomics (Sanford-Burnham-Prebys Medical Discovery Institute, La Jolla, CA). The screening was performed using a fully integrated automatic system using Stäubli TX90XL robotic arm (Pfäffikon, Swizerland), Labcyte Echo 555 acoustic dispenser (Sunnyvale, CA), Multidrop Combi reagent dispenser (Thermo Scientific, Waltham, MA), HighRes Pintool transfer device with ultrasonic bath (HighRes Biosolutions, Woburn, MA), Velocity 11 VSpin centrifuge (Agilent Technologies, Santa Clara, CA), and PheraStar FS plate reader (BMG LABTECH). The binding of at 25 μM library compounds to p32 protein was studied by their ability to displace FAM-TT1 from p32 protein. Peptide and protein were diluted immediately prior to screening, kept on ice during screening, and FAM-peptide was protected from light throughout the experiment.

Evaluation of concentration-dependence and specificity of the hit compounds

Results of the high-throughput screen were confirmed in dose response tests. 8.25 μM to 100 μM dilutions of the compounds that displaced FAM-peptide from p32 were used in competition with FAM-peptide as described in previous section. Specificity of the hit compounds was verified by examining their binding to a different protein, b1b2 domain of NRP-1 [5]. Experimental method for NRP-1 b1b2 was developed and validated similarly to p32, using FAM-RPARPAR peptide as a known peptide ligand for NRP-1. The displacement of FAM-RPARPAR from NRP-1 protein by the hit compounds was studied in 384-well format, as described above.

Phage binding and inhibition assay

The ability to inhibit TT1-phage binding to p32 protein was used as a secondary assay to verify the hit compounds. The competition assay was based on the phage binding assay described above with minor modifications. ELISA plates were coated with 2.5 µg/mL p32, incubated with phages ($1.11x10^8$ pfu in 100µL PBST) and 100 µM hit compounds at 4ºC overnight, and followed by antibody incubation and chromogenic reaction. Negative controls included DMSO at concentration it was used to dissolve the hit compounds.

NMR samples and data acquisition

All the NMR experiments were carried out on a Bruker Avance 700 spectrometer equipped with a TCI cryoprobe at T=293 K. For structure determinations, the peptide concentration was 100 µM in the NMR buffer in presence of 150 µM of $ZnCl_2$. One-dimensional (1D) 1H spectra were acquired with a spectral width of 8417.51 Hz, relaxation delay 1.0 s, 8k data points for acquisition and 16k for transformation.

Silver nanoparticle functionalization with #4014008 and binding to immobilized p32

Silver nanoparticles (AgNPs) with CF555 dye-labeled neutravidin coatings (555-Ag-NA) were prepared as described in Pang et al. 2014, with the difference that AgNPs were synthesized by citrate reduction [6] with a core size of ~30 nm Ag rather than polyvinylpyrrolidone reduction. An extinction of $1x10^{10}$ M-1 cm-1 at the 405 nm Ag plasmon peak was used to quantify the concentration of AgNPs. A biotinylated form of the #4014008 compound was prepared by reacting amine-reactive sulfo-NHS-LC-Biotin (Pierce Cat# 21335) with 6-fold molar excess of the free amine containing #4014008 in DMSO. The unpurified biotinylated product was loaded into the 555-Ag-NA, washed by centrifugation and brought up in PBS containing 0.05% Tween 20 (PBST). The resulting #4014008 -555-Ag-NA (401-Ag for short) was added to wells having pre-immobilized protein, either p32 or hexahistidine-tagged control protein N3A (His-control). Wells were prepared by incubating 96-well high-binding titer plates (Costar #3590 EIA/RIA) with 5 µg/mL protein in PBS overnight at 4°C followed by blocking with 1% bovine serum albumin in PBS for 1 h at room temperature, and washing three times with PBST. After incubation with nanoparticles at room temperature for 3 h, the wells were washed 3x with PBST and imaged by epifluorescence microscopy with a 20X objective (Leica DMIRE2). The number of particles per field of view

was then thresholded to remove the uniform background fluorescence and the number of nanoparticle dots was quantified by ImageJ (command: Analyze Particles).

Preparation of iron oxide nanoworms

NWs were prepared as previously described [7]. Aminated NWs were pegylated with maleimide-5K-PEG-NHS (JenKem Technology). #4014008 compound was conjugated to the nanoparticles through a thioether bond. The compound was modified to have a fluorescein and a cysteine thiol to aid the Michael addition between the compound and the maleimide-functionalized particles.

In vivo homing of iron oxide nanoworms

Animal experimentation was performed according to the procedures approved by the Animal Research Committee at the Sanford-Burnham-Prebys Medical Discovery Institute, San Diego. To generate breast tumors BALB/c nude mice were orthotopically injected with MCF10CA1a into the mammary fat pad with 2×10^6 cells suspended in 100 μL of PBS. Mice bearing orthotopic breast tumors were used for homing experiments when the tumors reached 0.5-1 cm in size. FAM labeled #4014008 -NWs were injected into the tail vein (7.5 mg of iron per kilogram of body weight), the animals were euthanized 5-6 hours after the injection by cardiac perfusion with PBS under anesthesia, and organs were dissected and analyzed for particle homing.

Immunofluorescence and immunohistochemistry

Tissues from mice injected with nanoparticles were fixed in 4% paraformaldehyde overnight at 4°C, cryoprotected in 30% sucrose overnight, and frozen in optimal cutting temperature (OCT) embedding medium.

For immunostaining, 7 μm thick tissue sections were first incubated for 1 hour at room temperature with 10% serum from the species in which the secondary antibody was generated, followed by incubation with the primary antibody overnight at 4°C. The following antibodies were used: rat monoclonal anti–mouse CD31 (1:50; BD Pharmingen) and rabbit p32 (1:250; Millipore). The primary antibodies were detected with Alexa 594 goat anti–rat and 594 goat anti–rabbit secondary antibodies (1:1000; Molecular Probes). Each staining experiment included sections stained only with secondary antibodies as negative controls. Nuclei were counterstained with DAPI diamidino-2-phenylindole (5 mg/mL; Molecular

Probes). The sections were mounted in gel/mount mounting medium (Biomeda) and viewed under a LSM 710 NLO Multiphoton Laser Point Scanning Confocal Microscope (Zeiss).

Supporting References

[1] P. P. Karmali, V. R. Kotamraju, M. Kastantin, M. Black, D. Missirlis, M. Tirrell, E. Ruoslahti, *Nanomed. -Nanotechnol. Biol. Med.*, 10.1016/j.nano.2008.07.007.

[2] T. Teesalu, K. N. Sugahara, E. Ruoslahti, *Methods Enzymol.*, 10.1016/B978-0-12-396962-0.00002-1.

[3] J. C. Owicki, *Journal of Biomolecular Screening*, 10.1177/108705710000500501.

[4] W. A. Lea, A. Simeonov, *Expert Opinion on Drug Discovery*, 10.1517/17460441.2011.537322.

[5] C. W. Vander Kooi, M. A. Jusino, B. Perman, D. B. Neau, H. D. Bellamy, D. J. Leahy, *Proc. Natl. Acad. Sci. U. S. A.*, 10.1073/pnas.0700043104.

[6] P. C. Lee, D. Meisel, *J. Phys. Chem.*, 10.1021/j100214a025.

[7] L. Agemy, D. Friedmann-Morvinski, V. R. Kotamraju, L. Roth, K. N. Sugahara, O. M. Girard, R. F. Mattrey, I. M. Verma, E. Ruoslahti, *Proc. Natl. Acad. Sci. U. S. A.*, 10.1073/pnas.1114518108.